

Experimental Study of Flow Effects of Solid Particles' Size in Porous Media

S. Akridiss, E. El Tabach, K. Chetehouna, N. Gascoin, M. S. Kadiri

Abstract—Transpiration cooling combined to regenerative cooling is a technique that could be used to cool the porous walls of the future ramjet combustion chambers; it consists of using fuel that will flow through the pores of the porous material consisting of the chamber walls, as coolant. However, at high temperature, the fuel is pyrolysed and generates solid coke particles inside the porous materials. This phenomenon can lead to a significant decrease of the material permeability and can affect the efficiency of the cooling system. In order to better understand this phenomenon, an experimental laboratory study was undertaken to determine the transport and deposition of particles in a sintered porous material subjected to steady state flow. The test bench composed of a high-pressure autoclave is used to study the transport of different particle size (35 μm , 42 μm and 50 μm) of silicone carbide (SiC) initially present at 0.25% of the overall volume of water into the grade 30 of bronze (thickness = 3 mm). The variations of SiC mass, which is trapped into the material, had been observed for $P_{\text{in}} = 2$ bar and $\dot{m} = 4$ g/s. The results, for the different conditions, are analyzed and compared. The effect of accumulation of particles has been noticed for the three sizes of particles. The increase in mass for different lapses of time has been also emphasized to notice the behavior of the plot of accumulation. This study focuses on the impact of the diameter of the injected particles on the reduction of the permeability. It is expected to be used by aerospace engineers in order to study the efficiency of the transpiration cooling technique.

Keywords—Experimental study, permeability, porous material, suspended particles.

I. INTRODUCTION

TRANSPORT of particulate suspensions and colloids in porous medium with particle capture occurs in numerous processes of chemical, petroleum, and aerospace engineering. For example, in future hypersonic flights, the transpiration cooling technique can serve to cool the walls of the combustor, which are porous [1], [2]. However, the coking activity due to the pyrolysis of the coolant fluid (endothermic fuel) generates ultrafine particles (carbon coke) [3], [4]. As the suspension (fuel and coke) flows through the porous material, suspended particles under the influence of various forces move towards material's porosities where they accumulate. Particles suspended in the fluid with sizes larger than the pore throats in the porous media may deposit on the surface of the

media, forming a cake. Accumulated mass reduces continuously the porosity of the material. It yields an increasing pressure drop of the material. This leads to a decrease in the permeability of the material over time [5]. When the pressure drop achieves the critical level, the material is blocked and must be replaced. In order to keep the porous material permeable, which guarantee long usage and an acceptable efficiency of the transpiration cooling method, one should produce an optimized porous material by examining experimentally the evolution of its permeability over time.

Many investigations on particles flow mechanism through porous media are available in the literature [6]-[14]. The process of suspension transport in porous media accompanied by particle capture in the pores is called deep bed filtration [15]-[19]. According to the clean-bed filtration theory, the flow of suspended micro-particles through porous media can be characterized by two important phenomena, the transport and the attachment [20]. The transport is defined as the movement of the particles to the grain surface (porous material) and is quantified by the single collector efficiency factor. The accumulation of the micro-particles inside the porous media is defined as the attachment phenomenon. The attachment of the particles to the grain surface is quantified by the collision efficiency factor. The other important process is aggregation, which occurs when suspended particles clump together and form different clusters [21]. These phenomena are the result of several forces and mechanisms depending on particle density and size [22]. Many studies in laboratory columns have been conducted in order to investigate the different parameters governing the transport of particles in natural porous media and artificially created porous materials [20], [21]. Other studies propose to use sintered porous materials for the strut structure in a scramjet combustion chamber to protect it from ablation [23]. Nevertheless, the literature survey indicates that the mechanism of particle intrusion into sintered porous materials is not known in sufficient way.

This paper presents an experimental laboratory study on the process of transport and deposition of micro particles in sintered porous material under moderate flow conditions. The effect of the size of the injected particles on the particles accumulation and deposition and permeability reduction is studied.

II. MATERIALS AND METHODS

A. Experimental Bench

In this study, an experimental setup is developed in order to evaluate the filtration properties of a sintered porous material

S. Akridiss, K. Chetehouna and N. Gascoin are in INSA Centre Val de Loire-Campus of Bourges, PRISME laboratory, France (corresponding author, phone: 0033681347457; e-mail: safaa.akridiss@insa-cvl.fr).

E. El Tabach is in the University of Orleans, IUT of Bourges, PRISME laboratory, France (e-mail: eddy.el-tabach@univ-orleans.fr).

S. Akridiss is in University Hassan 1, IPOS laboratory, 25000, Khouribga, Morocco.

M. S. Kadiri is in University Hassan 1, IPOS laboratory, 25000, Khouribga, Morocco (e-mail: kadirims@yahoo.fr).

injected with ultra-fine solid particles (Fig. 1). It consists of a pressurizing autoclave connected to a permeation cell via stainless steel tube. The high-pressure autoclave (equipped with an agitator) of 2 liters is used to mix a fixed concentration of micro particles with water. The regulated injection pressure of the mixture towards the permeation cell is ensured by a bottle of pure nitrogen, which is connected to the autoclave. The permeation cell, made of stainless steel, has a length of 50 mm and an external diameter of 40 mm. This cell is divided into a high-pressure chamber at the inlet and a low-pressure chamber at the outlet. It contains the studied porous material, which is inserted in the middle of several seals to insure the tightness and avoid the leakages inside the cell. Three pressure sensors measure respectively the inlet and outlet pressures of the cell, as well as that prevailing in the autoclave. In addition, a mass flow meter (Coriolis) is placed upstream of the cell. All sensors are connected to a data acquisition system (about 1 Hz, 16 bits and 48 channels) that helps recording the transient variations in measurement during the experiments. Several valves control the pressure in the autoclave and the flow rate. At the exit of the permeation cell,

an empty reservoir is placed in order to collect the exfiltrated suspended particles from the porous material. For each experiment, a well-known mixture of suspended particles is injected at an initial fixed flowrate and for a certain time (t).

The porous material sample has a diameter of 30 mm (active diameter of 16 mm). It is weighted before each experiment. After the experiment, the sample, with its external cake (i.e. deposition of particles at the surface of the material), is dried in a natural convection oven (Memmert UN55 Plus) at 120 °C for 2 hours and then weighted (m_i) using a precise mass balance (KERN ABT-100 5NM). Then, the sample is weighted again after the cake is wiped in order to determine the mass of particles trapped (accumulated) inside the porosities of the sample (m_a). The mass of the wiped cake (m_d) is then measured. These data are needed to determine the evolution of the permeability of the material sample over time. It should be noted that at the end of each test, all the components (autoclave, tubes and permeation cell) of the bench are cleaned before starting the next test. The methodology to determine the variation of the material permeability is detailed in the following section.

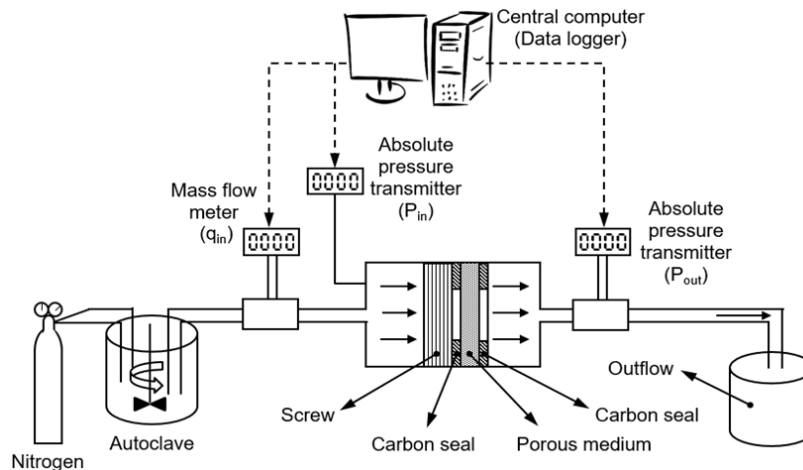


Fig. 1 Schematic diagram of the cell test

B. Darcy's Permeability Determination

Darcy's permeability of a material can be determined by several methods [24]-[27]. Many equations relate the permeability of a porous medium to the physical and geometrical properties of the solid skeleton such as porosity and tortuosity. However, it is complicated to determine the relationship to be used since it demands a meticulous knowledge of the porous structure and the connections inside the porous medium [28]. One of the most famous and simplest models for the permeability-porosity relationship is the Kozeny-Carman model [29], [30]. This model represents an attempt to describe permeability in terms of porosity. It is widely used in various fields such as ground water flow, chemical engineering, biochemical and medicine. In view of its practical limitations, the Kozeny-Carman equation has been frequently modified [31]-[35]. In this study, the Kozeny-Carman equation [29], [30] is used to determine the variation

of Darcy's permeability of the material due to accumulated particles inside its porosities. The theory proposed by Kozeny-Carman equation assumed that the porous medium is a bundle of capillaries of equal length and diameter and the flow is laminar and steady [36]. This equation can be written as:

$$K_D = \frac{d_g^2}{180} \times \frac{\epsilon^3}{(1-\epsilon)^2} \quad (1)$$

where d_g is the average grain diameter and ϵ is the porosity of the material. The porosity (ϵ) is a macroscopic property of a porous medium. This property is defined as the pore volume (V_{pore}) of a representative sample divided by its bulk volume (V_b). As it was mentioned, particle accumulation can change the pore morphology and consequently the porosity of porous media and the local pressure gradient. The change in porosity can be evaluated as:

$$\varepsilon = \varepsilon_0 - \frac{m_a}{V_b \times \rho_a} \quad (2)$$

where ε_0 is the initial porosity and ρ_p is the density of the accumulated particles.

If one assumes that the particle accumulation on the outside of the grains forms a relatively smooth surface on the grains, then a filter grain's effective diameter increases as the extent of accumulation increases. In this case, the change in the effective grain diameter (d_g) can be expressed [21] as:

$$\frac{d_g}{d_{g0}} = \left(\frac{1-\varepsilon}{1-\varepsilon_0} \right)^{1/3} \quad (3)$$

where d_{g0} is the initial grain diameter.

At the end of each experiment, the permeability of the material is calculated function of its initial properties and the accumulated mass particles inside the porosities of the material.

III. RESULTS AND DISCUSSION

A. Characterisation of the Porous Media and Particles

A metallic disk porous sample (Bronze) with a thickness of 3 mm has been considered. This sample comes from the supplier Sintertech Poral®. SEM visualization has been done on the sample (Fig. 2). The sample is composed of spheres with diameters ranging from 250 to 350 μm . The average value ($d_g=300 \mu\text{m}$) is taken in this study. The open porosity of the sample is estimated around 34%. The density (ρ_m) of the material is 8800 kg.m^{-3} .

Three different diameters of silicon carbide (SiC) particles were used: 35 μm , 42 μm , and 50 μm . These solid particles are chosen because they are immiscible to water, available in different diameters and safe to use. Their density is equal to 3210 kg.m^{-3} . In this study, the concentration of SiC in water is fixed to 0.25% (3.75g of SiC particles mixed to 1.5L of water). Moreover, the autoclave is pressurized in order to have an initial inlet mass flowrate of 4 g/s.

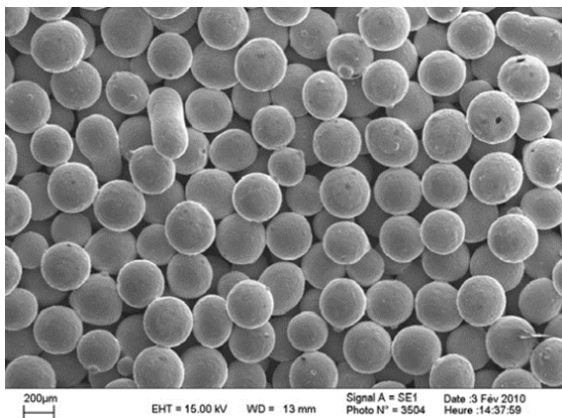


Fig. 2 SEM observation of the Bronze porous sample

B. Reliability Study

The reliability study is ensured in two ways. Indeed, the

initial calculated Darcy's permeability of the Bronze porous sample ($4.26 \times 10^{-11} \text{ m}^2$) using (1) is in good agreement with the value given by the manufacturer ($4.76 \times 10^{-11} \text{ m}^2$). This means that Kozeny-Carman equation can be applied in our case study. Moreover, each test is repeated at least three times in order to validate the reproducibility of the experimental results. The calculated maximum standard deviation for all the tests is less than 0.005, which is very satisfactory. For example, Table I gives the results of the repetition of a test where 3.75 g of SiC particles (35 μm) is mixed to 1.5 L of water in the autoclave that was pressurized in order to have an initial inlet mass flow rate of 4 g/s. The experiment plays out for 1 minute. The total mass (deposited on the surface and accumulated inside the porosities) and the accumulated mass (m_a) are found to be equal respectively to $0.21494 \pm 0.00259 \text{ g}$ and $0.18617 \pm 0.00254 \text{ g}$.

TABLE I
REPRODUCIBILITY QUANTIFIED ON PARTICLE MASS WEIGHT

Test	Total mass, m_t (g)	Accumulated mass, m_a (g)
Test 1	0.21446	0.18538
Test 2	0.21262	0.18902
Test 3	0.21775	0.18413

C. Effect of Particles Sizes and the Mass of Particles Accumulated Inside the Pores on the Darcy's Permeability of the Material

The measured mass of accumulated particles inside the porosities and the mass of the deposited cake for three different average diameters (35 μm , 42 μm , and 50 μm) of SiC particles at the end of each experiment are given respectively in Figs. 3 and 4. In comparison, the mass of the deposited particles on the surface of the porous material is proportionally greater than the mass of particles accumulated inside the porosities of the material for particles having a diameter of 42 μm and 50 μm . Fig. 3 shows that an increase in the particle diameter will lead to a decrease in the mass of deposited particles. It can be seen (Fig. 3) that, for both particles diameters of 42 μm and 50 μm , the stabilization time of the accumulated mass approximately corresponds to that for which the particles cake mass increases linearly (Fig. 4). This expected result shows that the developed test bench provides realistic results. It should be noted here that each test has been repeated at least three times. The maximum standard deviation value is less than 0.005.

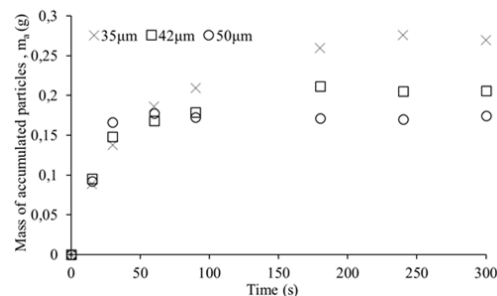


Fig. 3 Variation of accumulated particles mass function of time for all particles diameters

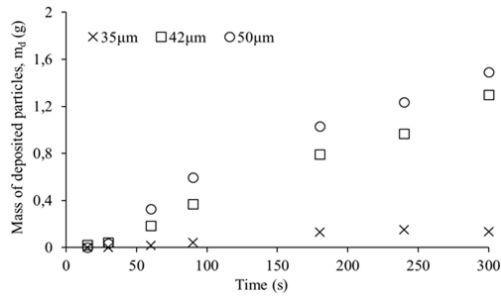


Fig. 4 Variation of deposited particles cake mass function of time for all particles diameters

Fig. 5 gives the evolution of the calculated Darcy's permeability of the studied material using Kozeny-Carman model (1) for all particles diameters. It can be observed that the Darcy's permeability decreases until a certain critical time t_c and, thereafter, the permeability will remain constant. This is due to the accumulation of particles inside the porosities of the material and to the deposition of the particles on its surface.

The critical times values for particles having average diameters of 35 μm , 42 μm and 50 μm are respectively 240 s, 180 s, and 90 s. The critical time decreases linearly when the average diameters of the particles increase.

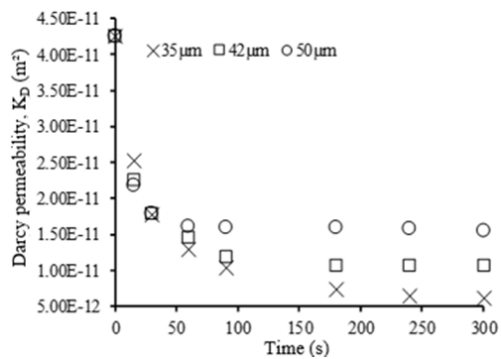


Fig. 5 Variation of calculated Darcy's permeability of the material function of time and of particles diameters

As the test time in the laboratory is not representative in the real configuration, the replacement of the time factor by another physical factor is necessary. In this study, the evolution of the porosity (ϵ) and the Darcy's permeability are studied as a function of mass of the deposited cake (Figs. 6 and 7). So, it is possible now to predict the porosity and the Darcy's permeability of the studied material by knowing the mass of deposited cake and the diameter of the injected particles. Like Fig. 5 and for all particles sizes, it can be observed that the porosity and the Darcy's permeability decreases until a certain critical m_d and, thereafter, the porosity and the permeability will remain constant. By applying the Kozeny-Carman equation to the tests results, it was concluded that the coefficient of permeability of the material specimen was decreased 3–7 times its initial value during injection as the porosity decreased. This important

result represents as an efficient indicator to better characterize the studied material

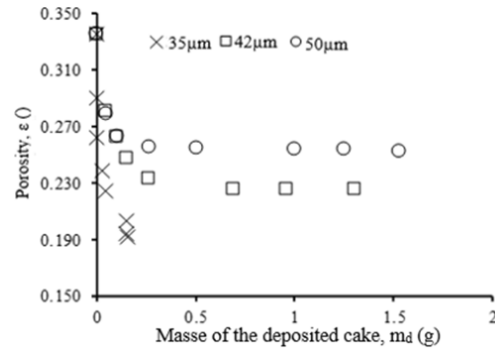


Fig. 6 Variation of the porosity of the material in function of the mass of deposited cake and of particles diameters

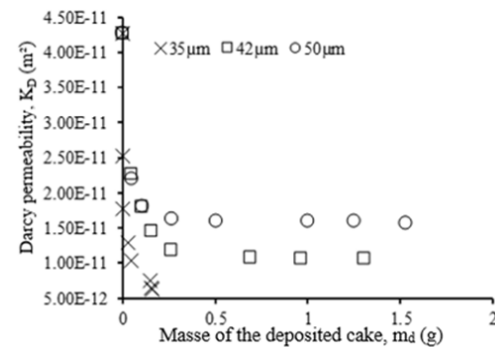


Fig. 7 Variation of Darcy's permeability of the material function of the mass of deposited cake and of particles diameters

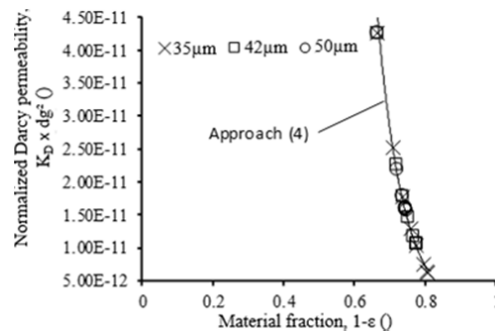


Fig. 8 Variation of normalized Darcy's permeability function of the solid material fraction for all particles diameters

The evolution of the normalized Darcy's permeability ($K_D \times d_g^{-2}$) as function of the solid material fraction ($1-\epsilon$) is given in Fig. 8. For the three different average particles diameters, it is found that the normalized Darcy's permeability data fit well (coefficient of determination equal to 0.99) to the following model:

$$\frac{K_D}{d_g^2} = 0.0077 \times e^{-0.0078 \times \rho_m \times (1-\epsilon)} \quad (4)$$

where ρ_m is the density of the studied material, kg.m^{-3} .

This model from (4) has been reported (with other coefficients) in the literature [37]. This proves once again the relevance of the results found. This model should help the engineering to better study the efficiency of the transpiration cooling technique.

IV. CONCLUSION

In this article, a new test bench has been developed in order to better understand the effect of the flow of suspended micro-particles through porous materials on its physical properties (porosity and permeability). The analysis of the obtained experimental data shows that the test bench gives accurate results. The obtained results should help the engineering study of material development and characterization to ensure optimum cooling efficiency. Other tests with different particles diameters, various mass flow rate and different material's thickness will be tested. Several permeabilities determination methods will be also compared in a near future.

ACKNOWLEDGMENT

The authors would like to sincerely thank D. Chocloff and A. Icardo from Naval academy of Brest for their technical and scientific support involving the computations and the experiments.

REFERENCES

- [1] T. Langener, J. Von Wolfersdorf, M. Selzer, and H. Hald, "Experimental investigations of transpiration cooling applied to C/C material," *Int. J. Therm. Sci.*, vol. 54, pp. 70–81, 2012.
- [2] G. Huang, Y. Zhu, Z. Liao, X.-L. Ouyang, and P.-X. Jiang, "Experimental investigation of transpiration cooling with phase change for sintered porous plates," *Int. J. Heat Mass Transf.*, vol. 114, pp. 1201–1213, 2017.
- [3] N. Gascoin, P. Gillard, S. Bernard, and M. Bouchez, "Characterisation of coking activity during supercritical hydrocarbon pyrolysis," *Fuel Process. Technol.*, vol. 89, no. 12, pp. 1416–1428, 2008.
- [4] E. El Tabach, L. Adishirinli, N. Gascoin, and G. Fau, "Prediction of transient chemistry effect during fuel pyrolysis on the pressure drop through porous material using artificial neural networks," *J. Anal. Appl. Pyrolysis*, vol. 115, pp. 143–148, 2015.
- [5] G. Fau, N. Gascoin, P. Gillard, M. Bouchez, and J. Steelant, "Fuel pyrolysis through porous media: Coke formation and coupled effect on permeability," *J. Anal. Appl. Pyrolysis*, vol. 95, pp. 180–188, 2012.
- [6] M. Elimelech, "Particle deposition on ideal collectors from dilute flowing suspensions: Mathematical formulation, numerical solution, and simulations," *Sep. Technol.*, vol. 4, no. 4, pp. 186–212, 1994.
- [7] R. Kretschmar, K. Barmettler, D. Grolimund, Y. Yan, M. Borkovec, and H. Sticher, "Experimental determination of colloid deposition rates and collision efficiencies in natural porous media," *Water Resour. Res.*, vol. 33, pp. 1129–1137, 1997.
- [8] T. Harter and S. Wagner, "Colloid Transport and Filtration of *Cryptosporidium parvum* in Sandy Soils and Aquifer Sediments," *Environ. Sci. Technol. - Env. SCI TECHNOL*, vol. 34, 1999.
- [9] N. Massei, M. Lacroix, H. Q. Wang, and J.-P. Dupont, "Transport of particulate material and dissolved tracer in a highly permeable porous medium: comparison of the transfer parameters," *J. Contam. Hydrol.*, vol. 57, no. 1, pp. 21–39, 2002.
- [10] A. Benamar, N.-D. Ahfir, H. Q. Wang, and A. Alem, "Particle transport in a saturated porous medium: pore structure effects," *C. R. Geosci.*, vol. 339, no. 10, pp. 674–681, 2007.
- [11] N. D. Ahfir, H. Q. Wang, A. Benamar, A. Alem, N. Massei, and J. P. Dupont, "Transport and deposition of suspended particles in saturated porous media: Hydrodynamic effect," *Hydrogeol. J.*, vol. 15, no. 4, pp. 659–668, 2007.
- [12] G. Kampel, G. H. Goldsztein, and J. C. Santamarina, "Particle transport in porous media: The role of inertial effects and path tortuosity in the velocity of the particles," *Appl. Phys. Lett.*, vol. 95, no. 19, pp. 2–4, 2009.
- [13] A. Lohne et al., "Formation-Damage and Well-Productivity Simulation," *SPE J. - SPE J*, vol. 15, pp. 751–769, 2010.
- [14] H. Fallah, H. B. Fathi, and H. Mohammadi, "The Mathematical Model for Particle Suspension Flow through Porous Medium," *Geomaterials*, vol. 2, no. 3, pp. 57–62, 2012.
- [15] A. C. Payatakes, R. Rajagopalan, and C. Tien, "Application of porous media models to the study of deep bed filtration," *Can. J. Chem. Eng.*, vol. 52, no. 6, pp. 722–731, 1974.
- [16] J. E. Altoé F., P. Bedrikovetsky, A. G. Siqueira, A. L. S. de Souza, and F. S. Shecaira, "Correction of basic equations for deep bed filtration with dispersion," *J. Pet. Sci. Eng.*, vol. 51, no. 1–2, pp. 68–84, 2006.
- [17] Z. You, Y. Osipov, P. Bedrikovetsky, and L. Kuzmina, "Asymptotic model for deep bed filtration," *Chem. Eng. J.*, vol. 258, pp. 374–385, 2014.
- [18] R. N. Sacramento et al., "Deep bed and cake filtration of two-size particle suspension in porous media," *J. Pet. Sci. Eng.*, vol. 126, pp. 201–210, 2015.
- [19] A. Vaz, P. Bedrikovetsky, P. D. Fernandes, A. Badalyan, and T. Carageorgos, "Determining model parameters for non-linear deep-bed filtration using laboratory pressure measurements," *J. Pet. Sci. Eng.*, vol. 151, no. September 2016, pp. 421–433, 2017.
- [20] R. May and Y. Li, "The effects of particle size on the deposition of fluorescent nanoparticles in porous media: Direct observation using laser scanning cytometry," *Colloids Surfaces A Physicochem. Eng. Asp.*, vol. 418, pp. 84–91, 2013.
- [21] A. Zamani and B. Maini, "Flow of dispersed particles through porous media - Deep bed filtration," *J. Pet. Sci. Eng.*, vol. 69, no. 1–2, pp. 71–88, 2009.
- [22] J. P. Herzig, D. M. Leclerc, and P. Le. Goff, "Flow of suspensions through porous media—Application to deep bed filtration," *Ind. Eng. Chem.*, vol. 62, 1970.
- [23] Y.-B. Xiong, Y.-H. Zhu, and P.-X. Jiang, "Numerical simulation of transpiration cooling for sintered metal porous strut of the Scramjet combustion chamber," *Heat Transf. Eng.*, vol. 35, no. 6–8, pp. 721–729, 2014.
- [24] H. C. Brinkman, "A calculation of the viscous force exerted by a flowing fluid in a dense swarm of particles," *Appl. Sci. Res.*, vol. 1, pp. 27–34, 1947.
- [25] H. Huang and J. A. Ayoub, "Applicability of the Forchheimer equation for Non-Darcy flow in porous media," *SPE Annual Technical Conference and Exhibition*, 2006, pp. 24–27.
- [26] N. Gascoin, G. Fau, P. Gillard, M. Kuhn, M. Bouchez, and J. Steelant, "Comparison of two permeation test benches and two determination methods for Darcy's and Forchheimer's permeabilities," *J. Porous Media*, vol. 15, no. 8, pp. 705–720, 2012.
- [27] E. El Tabach, N. Gascoin, M. Bouchez, and G. Fau, "Impact of post-processing methods on accuracy of darcian and forchheimer permeabilities determination," *J. Porous Media*, vol. 19, no. 9, pp. 771–782, 2016.
- [28] A. Rahmouni, A. Boulanouar, M. Boukalouch, Y. Géraud, A. Samaoui, M. Harnafi, J. Sebbani, "Relationships between porosity and permeability of calcarenite rocks based on laboratory measurements," *J. Mater. Environ. Sci.*, vol. 5, pp. 931–936, 2014.
- [29] J. Kozeny, "Ueber kapillare Leitung des Wassers im Boden," *Sitzungsber Akad. Wiss., Wien*, vol. 136 (2a), pp. 271–306, 1927.
- [30] P.C. Carman, "Fluid flow through granular beds". *Transactions, Institution of Chemical Engineers*, London, vol. 15, pp. 150–166, 1937.
- [31] G. Mavko and A. Nur, "The effect of a percolation threshold in the Kozeny-Carman relation," *Geophysics*, vol. 62, pp. 1480–1482, 1997.
- [32] C. H. Shih and J. Lee, "Effect of fiber architecture on permeability in liquid composite molding," *Polym. Compos.*, vol. 19, pp. 629–639, 1998.
- [33] E. Rodriguez, F. Giacomelli, and A. Vazquez, "Permeability-Porosity Relationship in RTM for Different Fiberglass and Natural Reinforcements," *J. Compos. Mater.*, vol. 38, no. 3, pp. 259–268, 2004.
- [34] P. Xu and B. Yu, "Developing a new form of permeability and Kozeny-Carman constant for homogeneous porous media by means of fractal geometry," *Adv. Water Resour.*, vol. 31, no. 1, pp. 74–81, 2008.
- [35] N. Henderson, J. C. Bréttas, and W. F. Sacco, "A three-parameter Kozeny-Carman generalized equation for fractal porous media," *Chem. Eng. Sci.*, vol. 65, no. 15, pp. 4432–4442, 2010.
- [36] J. Bear, *Dynamics of fluid in porous media*. Elsevier, New York, 1972.

- [37] R. E. Jordan, J. P. Hardy, F. E. Perron Jr, and D. J. Fisk, "Air permeability and capillary rise as measures of the pore structure of snow: an experimental and theoretical study," *Hydrol. Process.*, vol. 13, pp. 1733–1753, 1999.